Tree Physiology 37, 879–888
doi:10.1093/treephys/tpx086

Research paper

How well do growing season dynamics of photosynthetic capacity correlate with leaf biochemistry and climate fluctuations?

Danielle A. Way[1,2,4], Joseph R. Stinziano[1], Henry Berghoff[2] and Ram Oren[2,3]

[1]Department of Biology, University of Western Ontario, London, ON N6A 5B7, Canada; [2]Nicholas School of the Environment, Duke University, Durham, NC 27705, USA; [3]Xishuangbanna Tropical Botanical Garden, Chinese Academy of Sciences, Yunnan 666303, China; [4]Corresponding author (dway4@uwo.ca)

Received February 16, 2017; accepted June 7, 2017; published online July 4, 2017; handling Editor Lucas Cernusak

Accurate values of photosynthetic capacity are needed in Earth System Models to predict gross primary productivity. Seasonal changes in photosynthetic capacity in these models are primarily driven by temperature, but recent work has suggested that photoperiod may be a better predictor of seasonal photosynthetic capacity. Using field-grown kudzu (*Pueraria lobata* (Willd.) Ohwi), a nitrogen-fixing vine species, we took weekly measurements of photosynthetic capacity, leaf nitrogen, and pigment and photosynthetic protein concentrations and correlated these with temperature, irradiance and photoperiod over the growing season. Photosynthetic capacity was more strongly correlated with photoperiod than with temperature or daily irradiance, while the growing season pattern in photosynthetic capacity was uncoupled from changes in leaf nitrogen, chlorophyll and Rubisco. Daily estimates of the maximum carboxylation rate of Rubisco (V_{cmax}) based on either photoperiod or temperature were correlated in a non-linear manner, but V_{cmax} estimates from both approaches that also accounted for diurnal temperature fluctuations were similar, indicating that differences between these models depend on the relevant time step. We advocate for considering photoperiod, and not just temperature, when estimating photosynthetic capacity across the year, particularly as climate change alters temperatures but not photoperiod. We also caution that the use of leaf biochemical traits as proxies for estimating photosynthetic capacity may be unreliable when the underlying relationships between proxy leaf traits and photosynthetic capacity are established outside of a seasonal framework.

Keywords: day length, phenology, photosynthesis, remote sensing, seasonality, thermal acclimation.

Introduction

Estimates of photosynthetic capacity are critical for predicting terrestrial carbon fluxes through coupled vegetation–atmosphere models (Kattge et al. 2009, Oleson et al. 2013) and correlating remote sensing measurements with carbon fluxes (Ollinger et al. 2008). Many of these models estimate carbon fixation by using a base value of photosynthetic capacity, measured as the maximum carboxylation rate of Rubisco (V_{cmax}) or the maximum electron transport rate (J_{max}), for the plant functional type of interest and then assume that seasonal changes in V_{cmax} or J_{max} are primarily responsive to air temperature (Rogers et al. 2017). This assumption is based on well-established short-term temperature effects on Rubisco (Bernacchi et al. 2001) and electron transport (Bernacchi et al. 2003) kinetics, which promote photosynthetic capacity at higher leaf temperatures.

While the response of photosynthetic capacity to short-term temperature changes is clear, temperature may not be the best, or only, environmental factor correlated with changes in photosynthetic capacity across a year. For example, there is evidence that tree access to water and leaf water status are correlated with seasonal changes in photosynthetic capacity in oak species (Xu and Baldocchi 2003, Osuna et al. 2015). Recent work has also shown that photoperiod must be taken into account to correctly capture seasonal relationships between V_{cmax} and CO_2 fluxes at both the forest stand and global scales (Bauerle et al. 2012, Stoy et al. 2014). While there is currently no known

mechanistic link between changes in day length and variation in photosynthetic capacity, photoperiod is a reliable cue of seasonality and plants have evolved to use this cue to synchronize other plant traits, such as growth, flowering and leaf senescence, with the changing seasons (Amasino 2010, Gill et al. 2015, Way and Montgomery 2015). If photosynthetic capacity is indeed responding to photoperiod more than temperature, our predictions of V_{cmax} and J_{max} will be increasingly biased as the climate changes, since temperatures will warm while photoperiod will be unaffected, and temperature-based estimates of photosynthetic capacity will thus also increase, although photoperiod-based estimates of V_{cmax} and J_{max} would be unaltered.

Examining seasonal patterns of photosynthetic capacity requires data from frequent measurements of V_{cmax} and J_{max} made repeatedly on the same vegetation over a growing season. While there are few studies that measure V_{cmax} and J_{max} in this way across a growing season, even fewer study how these parameters relate to leaf biochemistry. Relationships between leaf nitrogen, chlorophyll and photosynthetic capacity are therefore often assumed to be relatively constant after the spring green-up and before leaf senescence begins in the autumn in deciduous, temperate species. While some variation in these relationships is expected, usually due to temporary environmental stress such as drought or extreme temperature (Grassi et al. 2005), and this variation is acknowledged in the literature (Evans 1989), the general constancy of these relationships underlies many modeling efforts, where a measurement of one leaf trait can be used to extrapolate to other leaf characteristics. For example, remote sensing techniques use spectral data to predict leaf chlorophyll concentrations (e.g., Inoue et al. 2016) and spectral signals related to chlorophyll concentrations can be extrapolated to leaf nitrogen (e.g., Inoue et al. 2012). These measurements are based on the assumption that leaf nitrogen concentrations are good proxies for photosynthetic performance, a relationship that is well-established in the literature (e.g., Field and Mooney 1986, Evans 1989, Reich et al. 1995, Ripullone et al. 2003, Grassi et al. 2005). However, often a single collection of leaf nitrogen (or some leaf physiological trait, such as net CO_2 assimilation rate, A_{net}) is made from a site in mid- to late summer to build these correlations of spectral data with leaf biochemistry and function (e.g., Martin et al. 2008, Ollinger et al. 2008, but see Dillen et al. 2012). As relationships between leaf spectral qualities (such as chlorophyll or carotenoid concentrations), leaf nitrogen content and leaf physiological activity vary over the growing season, relationships derived at one point in the year will not accurately predict leaf traits or activity at other times, even within a single plot.

To address these uncertainties, we measured weekly changes in photosynthetic capacity, leaf nitrogen and leaf biochemical traits in field-grown kudzu plants across a growing season. Kudzu (*Pueraria lobata* (Willd.) Ohwi), an invasive, nitrogen-fixing vine in North America, produces leaves throughout the growing season, only dropping them at the first frost, so newly expanded leaves developed over the entire experiment. As leaf age negatively correlates with photosynthetic capacity and leaf nitrogen in many species (Niinemets 2016), this enabled us to study seasonal signals in leaf physiology without the confounding effect of leaf age. We used this system to test the following hypotheses: (i) photosynthetic capacity (V_{cmax} and J_{max}) will be better correlated with changes in air temperature than with changes in photoperiod; and (ii) growing season changes in photosynthetic capacity measured repeatedly in the same plants would correlate with changes in leaf biochemistry, particularly Rubisco, chlorophyll and nitrogen concentrations, across the growing season.

Materials and methods

Twelve kudzu plants were grown from seed in pots in the Duke University Phytotron. Once established, the seedlings were planted in the field on 17 June 2011. The site consisted of an old-field with a clay-based soil in Durham County, NC, USA (36.0136416, -79.003928). Over the summer and autumn of 2011, competing grasses were trimmed back to facilitate kudzu establishment and the plants were watered every 2 days, unless it rained, to prevent water stress. Plants over-wintered in the field, re-emerging in May 2012, when regular watering and maintenance of the surrounding vegetation were reestablished. These 12 plants formed part of a larger study examining plant hydraulic traits, but this study focuses on the gas exchange and biochemistry of a subset of these plants.

Gas exchange

Measurements of photosynthetic capacity were made on fully-expanded, mature leaves near ground height (less than 1.5 m from the ground) approximately every week over the 2012 growing season (May to October). The aim was to repeatedly use the same plants over the experiment; due to deer herbivory, only four of the original six plants could be followed all season, and two new plants (of the 12 planted kudzu) were recruited to ensure six measurements per sampling day. Measurements were made between 8:00 and 13:00 h to ensure sufficient light to activate photosynthetic enzymes, but minimize exposure to high mid-summer temperatures and vapor pressure deficits. Responses of net CO_2 assimilation rates (A_{net}) to changes in intercellular CO_2 concentrations (C_i) were measured with a portable photosynthesis system (Li-Cor 6400, Li-cor, Lincoln, NE, USA). The cuvette maintained a leaf temperature of 30 °C, a saturating photosynthetic photon flux density of 1500 μmol m^{-2} s^{-1} [saturation assessed by light response curves (data not shown)], and a vapor pressure deficit of ~2.1 kPa. CO_2 concentrations began at 400 μmol mol^{-1}, were lowered step-wise to 50 μmol mol^{-1}, reset to 400 μmol mol^{-1} and then raised step-wise to 2000 μmol mol^{-1}; measurements were made once values were stable at each CO_2 concentration. Leaf temperature was held at 30 °C, rather than the more commonly used 25 °C,

because leaf temperatures of 30 °C could be attained in the field throughout the summer, but lower leaf temperatures were difficult to maintain during mid-summer in the field. Maximum rates of Rubisco carboxylation (V_{cmax}) and electron transport (J_{max}) were calculated (Farquhar et al. 1980) using temperature-corrected values of K_c, K_o and Γ^* from Bernacchi et al. (2001). Measured leaves were harvested after gas exchange measurements: half of each leaf was immediately frozen in liquid N_2 and stored at −80 °C, and the other half was measured for leaf area (Li-3100C, Li-cor) and then dried at 60 °C to constant mass for specific leaf area (SLA).

Climate data

Photoperiod was calculated for each measurement day based on site latitude. Climate data were taken from a tower at the Duke Free Air CO_2 Enrichment (FACE) site, ~10 km from the experiment. Air temperature above the forest canopy was measured every half-hour (HMP 35C, Vaisala, Helsinki, Flinland) and recorded with dataloggers. Photosynthetically active radiation (PAR) was measured above the forest canopy every 30 min with a quantum sensor (Li-190, Li-cor), and the half-hourly PAR records were summed over each day for an index of daily PAR. Mean, minimum and maximum air temperatures and mean daily summed PAR were calculated for the 24-h period prior to measurements (a 1-day lagged time period) and for similar 2-, 3-, 5-, 7- and 10-day timespans before each measurement day to assess potential lagged climate effects on photosynthetic performance.

Leaf biochemistry

Dried leaf material was finely ground for leaf nitrogen and carbon content analysis (Carlo-Erba NC2100 elemental analyzer, ThermoQuest Italia, Milan, Italy). The frozen leaf tissue was ground in liquid N_2 and divided into two subsamples, one for leaf pigment analysis and one for protein analysis. Pigments (total carotenoids, and chlorophyll *a* and *b*) were extracted from the first set of subsamples in methanol according to Busch et al. (2007) and quantified spectrophotometrically according to Wellburn (1994). Proteins were extracted and analyzed from the second set of subsamples, using a protocol based on Busch et al. (2007), by grinding in 2 ml of 4% SDS containing 3 mg ml^{-1} DTT per gram of leaf tissue using a Ten-Broeck glass homogenizer. Crude extracts were heated at 95 °C for 5 min then diluted twofold with loading buffer containing 4% SDS, 0.3 M Trizma base and bromophenol blue dye prior to SDS-PAGE. Proteins from crude extracts were separated on 12.5% polyacrylamide gels using SDS-PAGE modified from Laemmli (1970). Proteins were electrotransferred for 1 h at 100 V onto nitrocellulose membranes, which were then blocked with milk powder in Trizma-buffered saline (TBS) followed by three 5 min washes of TBS. Rabbit primary antibodies toward the Rubisco large subunit (gifted from N.P.A. Hüner) were diluted to 1:5000 and used to incubate blocked membranes for 1 h followed by four 10 min washes in TBS. Secondary goat antibodies toward rabbit proteins conjugated to horse radish protein (A6154, Sigma-Aldrich, Oakville, ON, Canada) were diluted 1:5000, and incubated with the membrane for 1 h, followed by four 10 min washes in TBS. Enhanced chemiluminescence reagent (RPN2109, GE Life Sciences, Mississauga, ON, Canada) was used to detect HRP antibodies on X-ray film. Rubisco large subunit standard (AS01 017S, Agrisera, Vännäs, Sweden) was used to create a standard curve to quantify Rubisco. Immunoblot bands were quantified against the Rubisco standard curve using ImageJ (NIH, Bethesda, MD, USA).

Statistics

Growing season changes in photosynthetic capacity, air temperature, daily PAR and photoperiod were all fit with third-order polynomials; the day of year (DOY) for peak values of each parameter was derived from these equations. Regressions were used to characterize relationships between measured parameters, leaf traits and climate data. We then used the best temperature predictors for V_{cmax} and J_{max}, along with photoperiod, leaf %N and SLA, to build a stepwise model to predict growing season changes in photosynthetic capacity. The minimum Bayesian Information Criterion was used to build all statistical models in a forwards direction [and using a backwards direction had no effect on the results (data not shown)]. Statistical analyses were performed with JMP Pro (version 10.0.0, SAS, Cary, NC, USA). All regressions and statistics were performed on raw data, and these results are stated in the text. However, figures show mean values where appropriate and the corresponding r^2 and *P*-values for the mean data are shown in these figures.

Results

Photosynthetic capacity, air temperature, daily PAR and photoperiod all increased in the early summer and then declined over the late summer and autumn (Figure 1). Photosynthetic capacity peaked in mid-summer, with V_{cmax} peaking on DOY 179 and J_{max} on DOY 173 (Figure 1B and C). Photoperiod peaked (summer solstice) on DOY 172 (Figure 1A) and daily PAR (which varies both with photoperiod and with cloud cover) peaked on DOY 175, while air temperature peaked over 3 weeks later, on DOY 195 (Figure 1A). Photosynthetic capacity thus peaked within a week of the longest day of the year, but 2–3 weeks before peak temperatures.

Photoperiod was a better predictor of photosynthetic capacity than the most highly correlated lagged air temperature parameter (Table 1). Changes in photoperiod explained more seasonal variation in the V_{cmax} data ($r^2 = 0.45$, $P < 0.0001$) than the best temperature parameter [1-day lagged mean air temperature (T_{air}); $r^2 = 0.34$, $P < 0.0001$] in the raw data (Figure 2A and

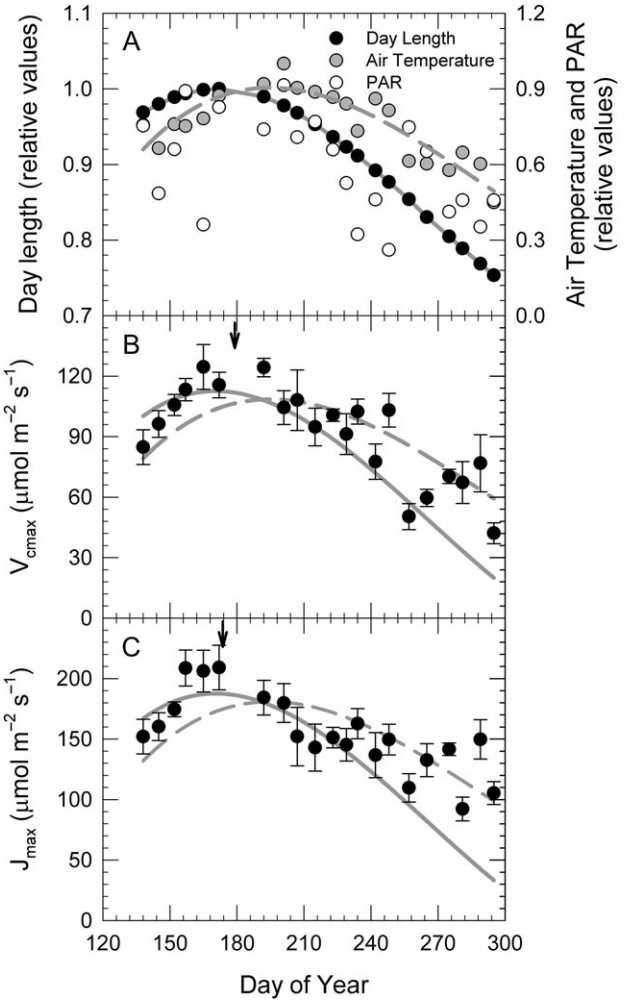

Figure 1. Growing season trajectories of climate and photosynthetic capacity. (A) Growing season photoperiod (black circles, solid line), 1-day lagged mean air temperature (gray circles, dashed line) and 1-day lagged daily PAR (empty circles), all relativized to the maximum value, with corresponding growing season changes in photosynthetic capacity measured as (B) V_{cmax} and (C) J_{max}. Photoperiod (solid line) and 1-day lagged mean air temperature (dashed line) are shown in (B) and (C) for reference. Arrows in (B) and (C) indicate estimated DOY for peak V_{cmax} (DOY 179) and J_{max} (DOY 173). Means ± SE for V_{cmax} and J_{max}, $n = 6$.

C). Similarly, photoperiod explained twice as much of the seasonal variability in J_{max} ($r^2 = 0.30$, $P < 0.0001$) as the 1-day lagged mean T_{air} (the best temperature predictor, $r^2 = 0.15$, $P < 0.0001$) across the measurements (Figure 2B and D). The 10-day lagged mean daily PAR was the best irradiance correlate with both V_{cmax} and J_{max} ($r^2 = 0.41$ and 0.26, respectively, $P < 0.0001$ for both), approaching, but not reaching, the explanatory power of photoperiod for photosynthetic capacity. However, mean daily PAR was increasingly correlated with photoperiod as the lag time increased (Table 2), such that the strong correlation of 10-day lagged mean daily PAR with photosynthetic capacity effectively reflects changes in photoperiod.

Table 1. Correlations of photosynthetic capacity (V_{cmax} and J_{max}) with lagged environmental parameters. Reported values are r^2 of linear regressions, P-values of regressions shown with asterisks: *<0.05; **<0.01; ***<0.0001.

	1-day lag	2-day lag	3-day lag	5-day lag	7-day lag	10-day lag
Photoperiod						
V_{cmax}	0.45***					
J_{max}	0.30***					
Mean T_{air}						
V_{cmax}	0.34***	0.32***	0.31***	0.30***	0.26***	0.27***
J_{max}	0.15***	0.12***	0.10**	0.08**	0.06*	0.07*
Minimum T_{air}						
V_{cmax}	0.33***	0.33***	0.30***	0.24***	0.21***	0.21***
J_{max}	0.14***	0.13***	0.09**	0.06**	0.04*	0.04*
Maximum T_{air}						
V_{cmax}	0.27***	0.29***	0.32***	0.29***	0.28***	0.29***
J_{max}	0.09**	0.09**	0.11**	0.09**	0.08**	0.09**
Mean daily PAR						
V_{cmax}	0.04*	0.04*	0.15***	0.26***	0.38***	0.41***
J_{max}	0.05*	0.04*	0.13***	0.21***	0.26***	0.26***

Responses of V_{cmax} and J_{max} to temperature are curvilinear when leaf temperatures approaching 40 °C are reached (Medlyn et al. 2002), so we also investigated whether a second-order polynomial fit was more appropriate than a linear regression for modeling the changes in photosynthetic capacity to temperature. Since simple linear regressions had similar explanatory power to the more complex curvilinear fits (V_{cmax} versus 1-day lagged mean T_{air}: polynomial $r^2 = 0.36$, linear $r^2 = 0.33$, both $P < 0.0001$; J_{max} versus 1-day lagged mean T_{air}: both $r^2 = 0.15$, $P < 0.0001$), linear regressions were used.

To determine whether there was a remnant signal from temperature in the photosynthetic capacity data once photoperiod was considered (and vice versa), we examined the residuals of the relationships shown in Figure 2. The lagged air temperature parameters did not explain variability in the residuals from the photoperiodic analyses of photosynthetic capacity ($P > 0.33$, Figure 3A and B). In contrast, photoperiod explained a significant proportion of variation in the residuals from the air temperature versus J_{max} analysis ($P < 0.05$, Figure 3D) and was close to being significantly correlated with the air temperature versus V_{cmax} residuals ($P = 0.052$, Figure 3C).

Despite concentrating on newly expanded leaves throughout the study, there was a 15% decline in the leaf nitrogen concentration over the growing season ($r^2 = 0.09$, $P < 0.001$; Figure 4A), from a regressed value of 3.35% on DOY 138 to 2.84% on DOY 295. Specific leaf area increased slightly over the growing season ($r^2 = 0.06$, $P < 0.005$; Figure 4B), which led to more pronounced declines in leaf nitrogen on an area basis over the year ($r^2 = 0.19$, $P < 0.0001$; Figure 4C). In contrast, there was no seasonal change in chlorophyll *a* or *b*,

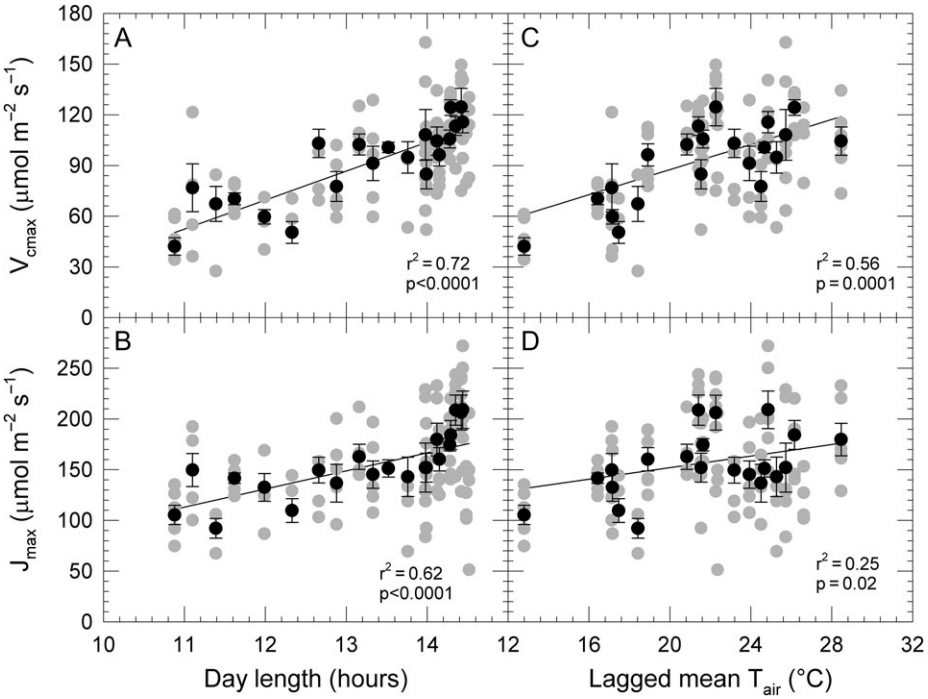

Figure 2. Relationship of photosynthetic capacity measured as V_{cmax} or J_{max} with photoperiod (A, B) or with the most significant temperature predictor. (C) V_{cmax} versus 1-day lagged mean air temperature; (D) J_{max} versus 1-day lagged mean air temperature. Black symbols indicate means ± SE, $n = 6$; gray symbols show raw data.

Table 2. Correlations of photoperiod with lagged mean daily PAR. Reported values are r^2 of linear regressions, P-values of regressions shown with asterisks: ***<0.0001.

	1-day lag	2-day lag	3-day lag	5-day lag	7-day lag	10-day lag
Photoperiod × PAR	0.25***	0.27***	0.45***	0.56***	0.85***	0.80***

carotenoid, or Rubisco concentrations per unit leaf area, or in the ratios of chlorophyll *a*:*b* (mean: 3.68 ± 0.03) and chlorophyll: carotenoids (mean: 4.83 ± 0.05) ($P > 0.1$ for all; Figure 5).

Leaf biochemical traits were weakly to moderately correlated with changes in photosynthetic capacity across the growing season, and were usually better correlated with post-solstice declines than with pre-solstice increases in V_{cmax} and J_{max}. Across all samples, the percent leaf nitrogen (%N) explained only 7–10% of the variation in photosynthetic capacity, measured as either V_{cmax} or J_{max} on a leaf area basis ($P < 0.005$), while area-based changes in leaf nitrogen explained slightly more variation in photosynthetic capacity (12–17%, $P < 0.0001$ for both V_{cmax} and J_{max}) (Figure 6A and D). However, when the data were divided into pre- and post-solstice periods, there was no significant relationship between leaf nitrogen (on either a mass or area basis) and either V_{cmax} or J_{max} ($0.29 < P < 0.79$) before mid-summer, while after the summer solstice, changes in leaf nitrogen explained 16–24% (V_{cmax}) and 18–24% (J_{max}) of the variation in photosynthetic capacity ($P < 0.0001$ for both). Total chlorophyll concentrations per unit leaf area were correlated with V_{cmax} ($r^2 = 0.21$, $P < 0.0001$) and J_{max} ($r^2 = 0.24$, $P < 0.0001$) across the growing season, but also explained less variation in pre-solstice photosynthetic capacity (V_{cmax}: $r^2 = 0.13$, $P = 0.035$; J_{max}: $r^2 = 0.19$, $P = 0.008$) than in post-solstice photosynthetic capacity (V_{cmax}: $r^2 = 0.29$, $P < 0.0001$; J_{max}: $r^2 = 0.39$, $P < 0.0001$) (Figure 6B and E). Rubisco concentrations per unit leaf area explained only 17% of the variation in V_{cmax} across the year ($P < 0.0001$), and a similar fraction of the variation in both pre- and post-solstice V_{cmax} (pre-solstice: $r^2 = 0.15$, $P = 0.02$; post-solstice: $r^2 = 0.19$ $P = 0.0005$; Figure 6C).

The stepwise model selected photoperiod as the only significant parameter for predicting growing season changes in V_{cmax} ($F = 102.7$, $P < 0.0001$), indicating that incorporating air temperature, leaf nitrogen or SLA did not significantly improve the model's ability to explain V_{cmax}. The model also selected photoperiod as the most significant predictor of J_{max} ($F = 47.5$, $P < 0.0001$), but indicated that incorporating SLA significantly improved the ability to capture seasonal changes in J_{max} ($F = 7.2$, $P < 0.01$). Overall, the J_{max} model with photoperiod and SLA explained 34% of the variation in measured J_{max} (compared with the 30% explained by photoperiod alone), while the V_{cmax}

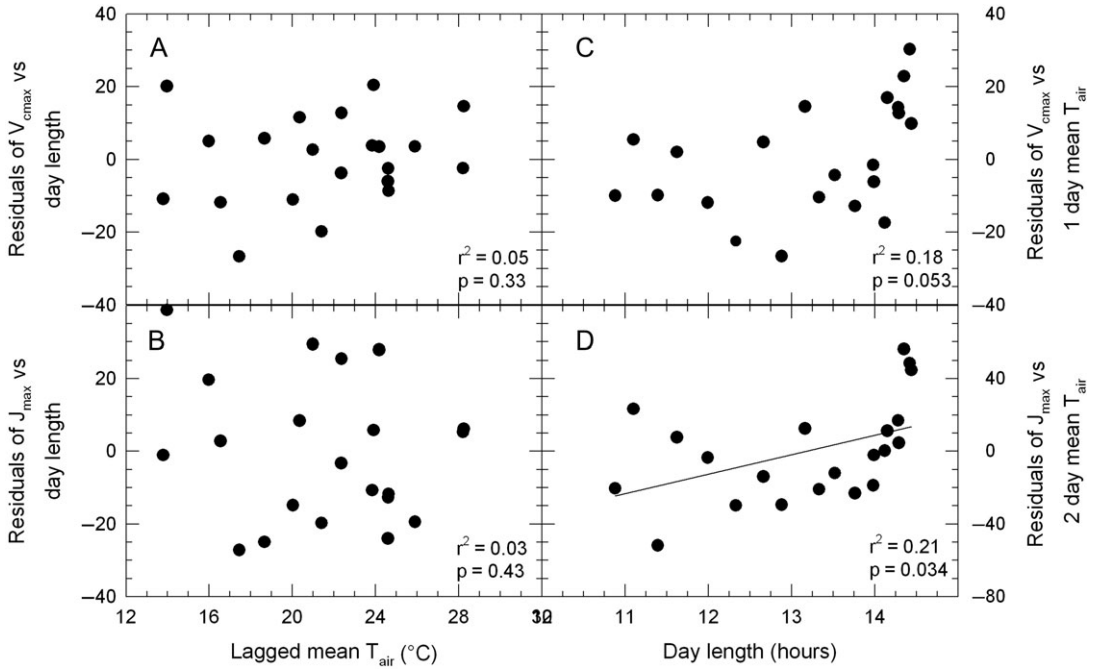

Figure 3. Relationship of residuals from Figure 2 plots with alternate climate parameters. (A) One-day lagged mean T_{air} versus residuals from V_{cmax}–photoperiod relationships (from Figure 2A); (B) 1-day lagged mean air temperature versus residuals from J_{max}–photoperiod relationships (from Figure 2B); (C) photoperiod versus residuals from V_{cmax}-lagged 1-day mean air temperature relationships (from Figure 2C); (D) photoperiod versus residuals from J_{max}-lagged 1-day mean air temperature relationships (from Figure 2D).

model explained 45% of the variability in V_{cmax} (the same value noted above for the relationship between individual V_{cmax} measurements and photoperiod).

Daily values for kudzu V_{cmax} were estimated for the field site from DOY 123 to 295 using the climate data from the site and both the photoperiod (Figure 2A) and the 1-day lagged mean temperature (Figure 2C) equations. At short photoperiods and cool temperatures, V_{cmax} estimated by photoperiod was lower than V_{cmax} calculated based on lagged temperature, but the opposite was true during mid-summer conditions (Figure 7A). These daily V_{cmax} values were then also temperature-corrected for diurnal temperature changes using half-hourly mean air temperature measurements at the field site and an activation energy of 65,330 J mol^{-1} for V_{cmax} from Bernacchi et al. (2001). When these daily V_{cmax} values from the photoperiod and lagged air temperature equations were scaled to reflect temperature variation within a day, the relationship between the V_{cmax} estimates from both approaches was linear, with a slope of 1.04 (Figure 7B).

Discussion

Temperature has been used to drive seasonal changes in photosynthetic capacity in coupled climate–vegetation models for years and is still the main factor dictating seasonal trajectories of V_{cmax} and J_{max} in most Earth System Models (Rogers et al. 2017). However, recent work has demonstrated the need to incorporate a photoperiodic scalar to estimate V_{cmax} across the year (Bauerle et al. 2012) and the importance of using this photoperiod correction at the ecosystem level (Stoy et al. 2014), leading to the incorporation of a photoperiod scalar in at least one Earth System Model (Oleson et al. 2013). The need to determine whether photoperiod effects on photosynthetic capacity should be broadly accounted for in Earth System Models has recently been acknowledged (Rogers et al. 2017), but there is little data available to meet this need. While there are a few experiments directly manipulating both temperature and photoperiod (e.g., Bauerle et al. 2012, Stinziano and Way 2017), we also need to assess this question with plants in a natural environment, where determining the driving factor may be less certain due to the covariance of photoperiod and air temperature, but the setting is ecologically realistic.

Here, we show that in contrast to our first hypothesis, photoperiod is a stronger predictor of seasonal V_{cmax} and J_{max} than air temperature in field-grown kudzu. In fact, photosynthetic capacity peaked and began declining within days of the peak and subsequent decline of photoperiod, during a period when temperatures were still increasing, emphasizing that decreases in V_{cmax} and J_{max} started 2–3 weeks before temperatures began to cool, consistent with the relative timing of declines in photoperiod, photosynthetic capacity and air temperature in Bauerle et al. (2012). Furthermore, as demonstrated in the residuals analyses in Figure 3, photosynthetic capacity estimates based on temperature were improved by considering photoperiod, while the reverse was not true, implying

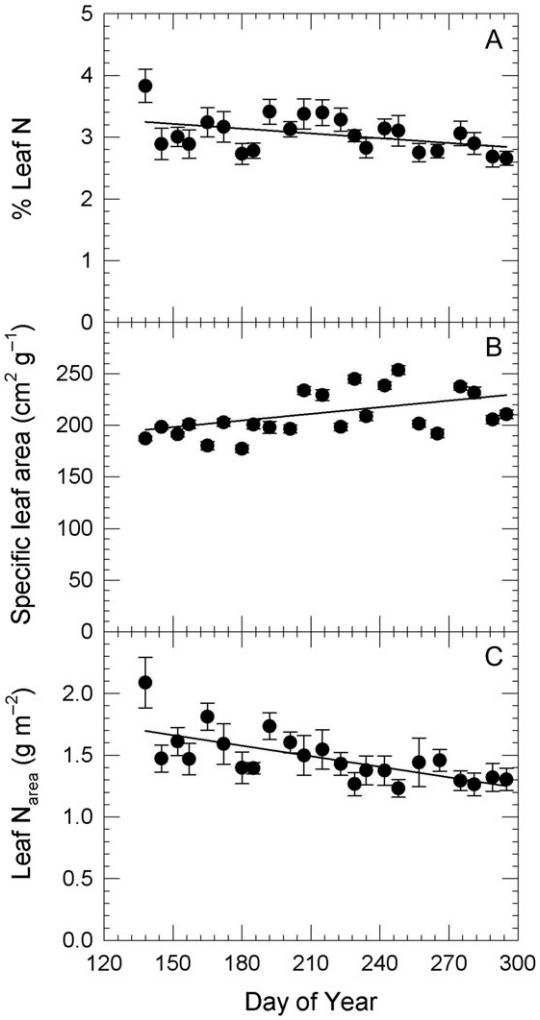

Figure 4. Growing season variation in (A) the percent leaf nitrogen, (B) the specific leaf area, and (C) leaf nitrogen on an area basis (N_{area}) of kudzu leaves. Means ± SE, $n = 6$.

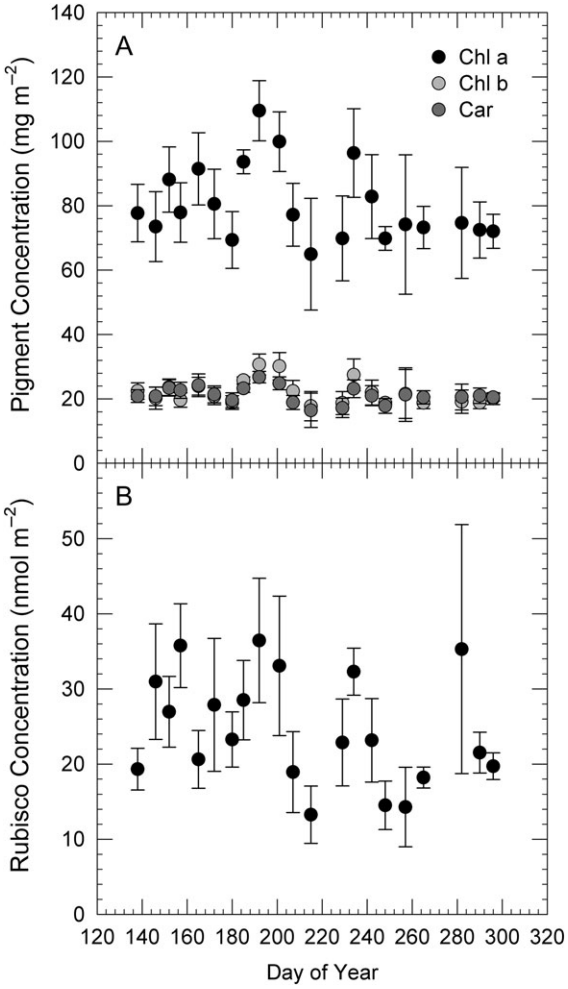

Figure 5. Growing season variation in (A) chlorophyll (chl) *a*, chl *b* and carotenoid (car) concentrations, and (B) Rubisco concentrations in kudzu leaves. Means ± SE, $n = 2–6$.

that there was a remnant photoperiodic signal in the photosynthetic capacity data even after temperature was accounted for. While daily V_{cmax} values estimated from a temperature approach and a photoperiod approach differed considerably over the growing season for our field site, differences between these two approaches were reduced when diurnal air temperature variation effects were superimposed on these V_{cmax} estimates (Figure 7). Thus, the need to incorporate photoperiod signals in current estimates of V_{cmax} may depend on the temporal resolution at which photosynthetic capacity is being modeled, although there was still a 4% difference between the two approaches even in the sub-daily estimates. However, as seasonal changes in photoperiod remain constant in the future while warming increases temperatures, the decoupling of the timing of these seasonal cues will mean that estimates of photosynthetic capacity based on photoperiod or daily temperatures will increasingly diverge in a warmer world.

In agreement with our second hypothesis, growing season changes in photosynthetic capacity were significantly correlated with changes in percent leaf nitrogen, leaf pigment concentrations and Rubisco concentrations. However these variables only explained 7–24% of the variation in V_{cmax} and J_{max} across the year. While the percent leaf nitrogen declined linearly by 15% from mid-May to October, and pigment and Rubisco concentrations remained relatively constant over time, photosynthetic capacity peaked in mid-June and showed a pronounced decline after the summer solstice. Both V_{cmax} and J_{max} decreased to ~50% of their peak mid-summer values by the end of October, which is a less dramatic decline than the 70–90% suppression of peak photosynthetic capacity seen in a range of temperate trees in Bauerle et al. (2012) for the same date. Thus, although photosynthetic capacity was broadly correlated with leaf traits, such as leaf nitrogen and chlorophyll concentration, that are commonly used as proxies for estimating carbon uptake, seasonal changes in the strength of the relationships between photosynthetic capacity and these leaf traits confound our ability to estimate V_{cmax} and J_{max} from measurements of these proxies over time. Wilson et al. (2000) also found that seasonal profiles in leaf nitrogen

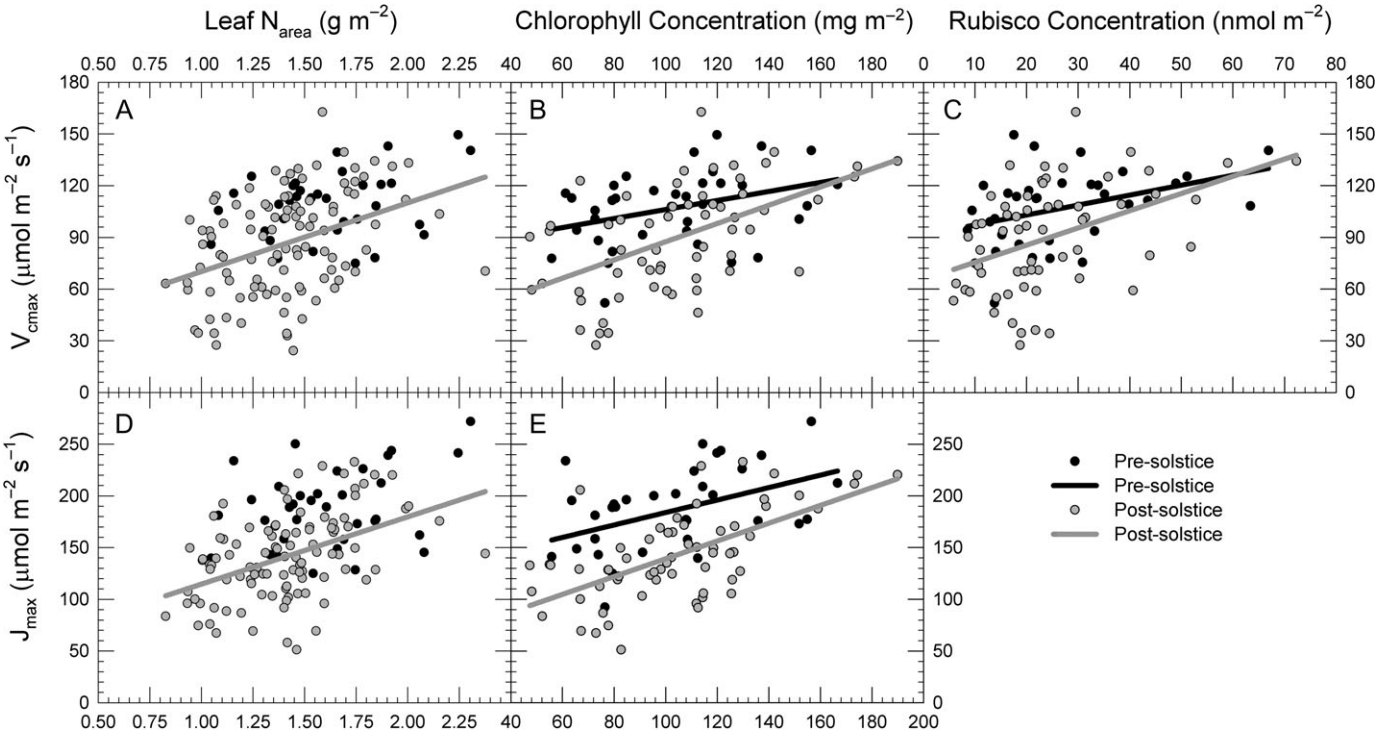

Figure 6. Relationship between photosynthetic capacity (V_{cmax}: A, B, C; J_{max}: D, E) and leaf nitrogen on an area basis (N_{area}) (A, D), chlorophyll concentration (B, E), and Rubisco concentration (D) in kudzu leaves. Black symbols and lines indicate data from before the summer solstice, while gray symbols and lines indicate post-solstice data. Lines indicate significant linear regressions, see text for details.

and V_{cmax} were not well correlated in deciduous tree species, and speculated that this may have been due to a reduced allocation of nitrogen to Rubisco in late summer and early autumn. However in our data, Rubisco concentrations were fairly constant across the growing season and the correlation between Rubisco concentrations and V_{cmax} was only 19% after midsummer, indicating that the decline in V_{cmax} we see after the summer solstice is not solely attributable to decreases in Rubisco. Instead, there may be decreases in the activation state of Rubisco or reductions in mesophyll conductance as the summer progresses, both of which would decrease V_{cmax} without altering leaf nitrogen or Rubisco concentrations. Regardless of the mechanism responsible for the late summer decline in V_{cmax}, our work indicates that traditional leaf traits used as proxies for determining carbon uptake in vegetation from remote sensing, such as leaf pigment concentrations, did not provide robust estimates of photosynthetic performance across the growing season, although the correlations were stronger in the late summer. Indeed, recent work on remote sensing proxies has focused on solar-induced fluorescence as a proxy for net CO_2 uptake, as fluorescence predicts seasonal variation in photosynthesis better than do proxies based on plant structure or chlorophyll (Yang et al. 2015, Zarco-Tejada et al. 2016). As our plants were kept well-watered to prevent water stress, our results also do not capture any effect of leaf water status on photosynthetic capacity over the growing season, which may be an important consideration for capturing seasonal trajectories of V_{cmax} and J_{max} in some species, such as Mediterranean oaks, in a field-setting (Xu and Baldocchi 2003, Osuna et al. 2015).

Our data also imply that photosynthetic capacity in kudzu does not acclimate strongly to temperature. In all analyses, the 1-day lagged mean temperature was most tightly correlated with weekly measurements of V_{cmax} and J_{max}. While this could indicate that photosynthetic capacity was constantly acclimating to recent prevailing temperatures, the difference between the best and worst lagged temperature parameters was only ~7%, so even using a 10-day lagged temperature value produced similar estimates of V_{cmax} and J_{max} as did the 1-day lagged mean temperature. This general lack of responsiveness of photosynthetic capacity to recent growth temperature is consistent with meta-analyses that have found no relationship between V_{cmax} measured at a common temperature (e.g., 25 °C) and the growth temperature of the plant (Way and Oren 2010, Way and Yamori 2014). Given the recent push for including temperature acclimation into Earth System Models (Smith and Dukes 2013, Lombardozzi et al. 2015, Rogers et al. 2017), it will be important to determine how photosynthetic capacity acclimates to temperature, to prevent the introduction of large errors in estimates of gross primary productivity.

It remains unclear whether the correlation of variation in photosynthetic capacity and photoperiod across the growing season holds across a broad range of plant functional types. The

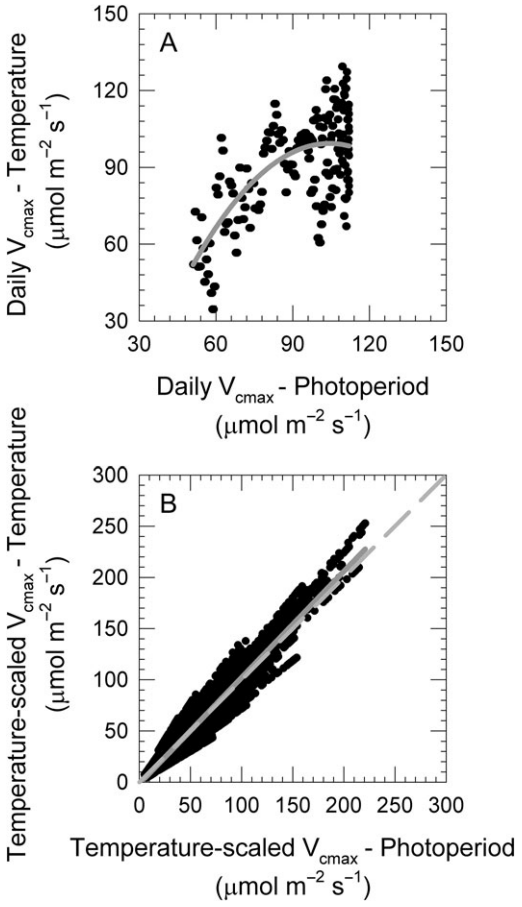

Figure 7. Relationships between (A) daily V_{cmax} estimated by photoperiod (from Figure 2A) and daily V_{cmax} estimated by 1-day lagged mean air temperature (from Figure 2C) and (B) V_{cmax} estimated by photoperiod and V_{cmax} estimated by 1-day lagged mean air temperature, where daily V_{cmax} values from (A) were temperature-scaled to 30-min field temperature variations for the growing season. Solid gray lines indicate regressions; dashed gray line indicates a 1:1 relationship in (B).

initial finding that day length was a better predictor of V_{cmax} and J_{max} than was temperature was limited to temperate, deciduous broad-leaved trees (Bauerle et al. 2012). Our work indicates that the same is true in a species from at least one other plant functional type, namely a winter deciduous, woody vine. In contrast to these deciduous species, manipulative experiments in two evergreen conifer species (*Picea abies* and *Picea glauca*) have shown that temperature, and not photoperiod, controls growing season changes in photosynthetic capacity (Stinziano et al. 2015, Stinziano and Way 2017). While the mechanisms controlling the seasonality of photosynthetic capacity are not well understood, there may be differences in the environmental signals used by evergreen and deciduous species or temperate and tropical species, for regulating photosynthetic performance over the growing season, particularly since evergreen leaves are kept for more than a single growing season and tropical species do not experience strong changes in photoperiod across the year. These issues, and the mechanisms underlying how photoperiod might influence photosynthetic capacity, warrant further research.

Acknowledgments

Judson Edeburn and the Duke Forest staff were invaluable in setting up the site. We thank Yanqun Zhang, Zong-dong Hou and Pantana Tor-Ngorn for help in growing the plants, and in planting and maintaining the experiment.

Conflict of interest

None declared.

Funding

This work was supported by grants from the US Department of Agriculture, Agriculture and Food Research Initiative (#2011-67,003-30,222), the US Department of Energy, Terrestrial Ecosystem Sciences (#11-DE-SC-0,006,967), and the US-Israeli Binational Science Foundation to D.A.W. and R.O. It was also supported by a Natural Sciences and Engineering Research Council of Canada (NSERC) Discovery grant and an Ontario Early Researcher Award to D.A.W., and an NSERC CGS-D Doctoral Scholarship to J.R.S.

References

Amasino R (2010) Seasonal and developmental timing of flowering. Plant J 61:1001–1013.

Bauerle WL, Oren R, Way DA, Qian SS, Stoy PC, Thornton PE, Bowden JD, Hoffman FM, Reynolds RF (2012) Photoperiodic regulation of the seasonal pattern of photosynthetic capacity and the implications for carbon cycling. Proc Natl Acad Sci USA 109:8612–8617.

Bernacchi CJ, Singsaas EL, Pimental C, Portis AR Jr, Long SP (2001) Improved temperature response functions for models of Rubisco-limited photosynthesis. Plant Cell Environ 24:253–259.

Bernacchi CJ, Pimental C, Long SP (2003) *In vivo* temperature response functions of parameters required to model RuBP-limited photosynthesis. Plant Cell Environ 26:1419–1430.

Busch FA, Hüner NPA, Ensminger I (2007) Increased air temperature during simulated autumn conditions does not increase photosynthetic carbon gain but affects the dissipation of excess energy in seedlings of the evergreen conifer Jack pine. Plant Physiol 143:1242–1251.

Dillen SY, Op de Beeck M, Hufkens K, Buonanduci M, Phillips NG (2012) Seasonal patterns in foliar reflectance in relation to photosynthetic capacity and color index in two co-occurring tree species, *Quercus rubra* and *Betula papyrifera*. Agric For Meterol 160:60–68.

Evans JR (1989) Photosynthesis and nitrogen relationship in leaves of C3 plants. Oecologia 78:9–19.

Farquhar GD, von Caemmerer S, Berry JA (1980) A biochemical model of photosynthetic CO_2 assimilation in leaves of C3 species. Planta 149:78–90.

Field CB, Mooney HA (1986) The photosynthesis-nitrogen relationship in wild plants. In: Givnish TJ (ed) On the economy of plant form and function. Cambridge University Press, Cambridge, UK, pp 25–55.

Gill AL, Gallinat AS, Sanders-DeMott R, Rigden AJ, Gianotti DJS, Mantooth JA, Templer PH (2015) Changes in autumn senescence in northern hemisphere deciduous trees: a meta-analysis of autumn phenology studies. Ann Bot (Lond) 116:875–888.

Grassi G, Vicinelli E, Ponti F, Cantoni L, Magnani F (2005) Seasonal and interannual variability of photosynthetic capacity in relation to leaf nitrogen in a deciduous forest plantation in northern Italy. Tree Physiol 25:349–360.

Inoue Y, Sakaiya E, Zhu Y, Takahashi W (2012) Diagnostic mapping of canopy nitrogen content in rice based on hyperspectral measurements. Remote Sens Environ 126:210–221.

Inoue Y, Guerif M, Baret F, Skidmore A, Gitelson A, Schlerf M, Darvishzadeh R, Olioso A (2016) Simple and robust methods for remote sensing of canopy chlorophyll content: a comparative analysis of hyperspectral data for different types of vegetation. Plant Cell Environ 39:2609–2623.

Kattge J, Knorr W, Raddatz T, Wirth C (2009) Quantifying photosynthetic capacity and its relationship to leaf nitrogen content for global-scale terrestrial biosphere models. Glob Chang Biol 15:976–991.

Laemmli UK (1970) Cleavage of structural proteins during the assembly of the head of bacteriophage T4. Nature 227:680–685.

Lombardozzi DL, Bonan GB, Smith NG, Dukes JS, Fisher RA (2015) Temperature acclimation of photosynthesis and respiration: a key uncertainty in the carbon cycle-climate feedback. Geophys Res Lett 42:8624–8631.

Martin ME, Plourde LC, Ollinger SV, Smith M-L, McNeil BE (2008) A generalizable method for remote sensing of canopy nitrogen across a wide range of forest ecosystems. Remote Sens Environ 112:3511–3519.

Medlyn BE, Dreyer E, Ellsworth D et al. (2002) Temperature response of parameters of a biochemically based model of photosynthesis. II. A review of experimental data. Plant Cell Environ 25: 1167–1179.

Niinemets U (2016) Leaf age dependent changes in within-canopy variation in leaf functional traits: a meta-analysis. J Plant Res 129: 313–338.

Ollinger SV, Richardson AD, Martin ME et al. (2008) Canopy nitrogen, carbon assimilation, and albedo in temperate and boreal forests: functional relations and potential climate feedbacks. Proc Natl Acad Sci USA 105:19336–19341.

Oleson KW, Lawrence DM, Bonan GB et al. (2013) Technical description of version 4.5 of the Community Land Model (CLM). National Center for Atmospheric Research, Boulder, CO, USA.

Osuna JL, Baldocchi DD, Kobayashi H, Dawson TE (2015) Seasonal trends in photosynthesis and electron transport during the Mediterranean summer drought in leaves of deciduous oaks. Tree Physiol 35:485–500.

Reich PB, Walters MB, Kloeppel BD, Ellsworth DS (1995) Different photosynthesis-nitrogen relations in deciduous hardwood and evergreen coniferous tree species. Oecologia 104:24–30.

Ripullone F, Grassi G, Lauteri M, Borghetti M (2003) Photosynthesis-nitrogen relationships: interpretation of different patterns between *Pseudotsuga menziesii* and *Populus* x *euroamericana* in a mini-stand experiment. Tree Physiol 23:137–144.

Rogers A, Medlyn BE, Dukes JS et al. (2017) A roadmap for improving the representation of photosynthesis in Earth System Models. New Phytol 213:22–42.

Smith NG, Dukes JS (2013) Plant respiration and photosynthesis in global-scale models: incorporating acclimation to temperature and CO_2. Glob Chang Biol 19:45–63.

Stinziano JR, Way DA (2017) Autumn photosynthetic decline and growth cessation in seedlings of white spruce are decoupled under warming and photoperiod manipulations. Plant Cell Environ. doi:10.1111/pce.12917.

Stinziano JR, Hüner NPA, Way DA (2015) Warming delays autumn declines in photosynthetic capacity in Norway spruce (*Picea abies*). Tree Physiol 35:1303–1313.

Stoy PC, Trowbridge AM, Bauerle WL (2014) Controls on seasonal patterns of maximum ecosystem carbon uptake and canopy-scale photosynthetic light response: contributions from both temperature and photoperiod. Photosynth Res 119:49–64.

Way DA, Montgomery RA (2015) Photoperiod constraints on tree phenology, performance and migration in a warming world. Plant Cell Environ 38:1725–1736.

Way DA, Oren R (2010) Differential responses to increased growth temperatures between trees from different functional groups and biomes: a review and synthesis of data. Tree Physiol 30:669–688.

Way DA, Yamori W (2014) Thermal acclimation of photosynthesis: on the importance of adjusting our definitions and accounting for thermal acclimation of respiration. Photosynth Res 119:89–100.

Wellburn AR (1994) The spectral determination of chlorophyll a and chlorophyll b, as well as total carotenoids, using various solvents with spectrophotometers of different resolution. J Plant Physiol 144:307–313.

Wilson KB, Baldocchi DD, Hanson PJ (2000) Spatial and seasonal variability of photosynthetic parameters and their relationship to leaf nitrogen in a deciduous forest. Tree Physiol 20:565–578.

Xu L, Baldocchi DD (2003) Seasonal trend of photosynthetic parameters and stomatal conductance of blue oak (*Quercus douglasii*) under prolonged summer drought and high temperature. Tree Physiol 23: 865–877.

Yang X, Tang J, Mustard JF, Lee J-E, Rossini M, Joiner J, Munger JW, Kornfield A, Richardson AD (2015) Solar-induced chlorophyll fluorescence that correlates with canopy photosynthesis on diurnal and seasonal scales in a temperate deciduous forest. Geophys Res Lett 42: 2977–2987.

Zarco-Tejada PJ, Gonzalez-Dugo MV, Fereres E (2016) Seasonal stability of chlorophyll fluorescence quantified from airborne hyperspectral imagery as an indicator of net photosynthesis in the contect of precision agriculture. Remote Sens Environ 179:89–103.